scientific reports

Check for updates

OPEN

Mesenchymal stem cell implantation mitigates ionizing radiation-induced vascular damage in the murine aorta

Toshio Uchiki[1,5], Nobuyuki Hamada[2✉], Asuka Fujita[1,5], Ki-ichiro Kawano[1], Seiko Hirota[3], Makoto Maeda[4], Ayano Sasaki[5], Shogo Nagamatsu[5], Shinji Yoshinaga[3], Ayumu Nakashima[6✉] & Yukihito Higashi[1✉]

For preparedness for some scenarios such as unintentional accidents or intentional malicious events, it is of critical importance to develop effective medical countermeasures against normal tissue injury from exposure to ionizing radiation. To this end, agents that are effective when administered after radiation exposure need to be developed. Considering that vascular injury is among the upstream events of radiation toxicity in various tissues, the present study was undertaken to investigate whether post-irradiation implantation of human mesenchymal stem/stromal cells (MSCs) restore vascular injury induced by acute irradiation. MSCs were obtained from human adipose tissue. For in vivo experiments, young adult male C57BL/6J mice ($n = 8$/group) were received intravenous injection of 5×10^4 MSCs or vehicle at 6 h after irradiation with 5 Gy (sublethal dose) of ^{137}Cs γ-rays. Control mice were sham-irradiated and received vehicle injection. At four weeks after irradiation, the aorta was collected, and subjected to scanning electron microscopy, immunofluorescence and histochemistry staining. Irradiation led to various changes in the aorta of mice, such as detachment and partial loss of the endothelium, decreases in vascular endothelial cadherin and endothelial nitric oxide synthase, vascular endothelial and smooth muscle cell death, inflammation (evidenced by increases in CD68, F4/80 and CD3) and fibrosis (evidenced by increases in transforming growth factor β1 and collagen). Post-irradiation MSC implantation restored such radiation-induced vascular damage.

Keywords Ionizing radiation, Mesenchymal stem cells, Vascular damage

Abbreviations

DAPI	4',6-diamidino-2-phenylindole
eNOS	Endothelial nitric oxide synthase
FE-SEM	Field-emission scanning electron microscopy
IMT	Intima-media thickness
IMT-HC	Intima-media thickness measured from histochemistry images
IMT-IF	Intima-media thickness measured from immunofluorescence images
MSC	Mesenchymal stem/stromal cell
MSC-CM	Mesenchymal stem/stromal cell-conditioned medium
PBS	Phosphate-buffered saline
TGF-β1	Transforming growth factor β1
VEC	Vascular endothelial cell

[1]Department of Regenerative Medicine, Division of Radiation Medical Science, Research Institute for Radiation Biology and Medicine, Hiroshima University, 1-2-3 Kasumi, Minami-ku, Hiroshima 734-8551, Japan. [2]Biology and Environmental Chemistry Division, Sustainable System Research Laboratory, Central Research Institute of Electric Power Industry (CRIEPI), Chiba 270-1194, Japan. [3]Department of Environmetrics and Biometrics, Division of Radiation Basic Science, Research Institute for Radiation Biology and Medicine, Hiroshima University Hospital, Hiroshima 734-8553, Japan. [4]Natural Science Center for Basic Research and Development, Hiroshima University, Hiroshima 739-8526, Japan. [5]Department of Plastic Surgery, Hiroshima University Hospital, Hiroshima 734-8553, Japan. [6]Department of Nephrology, Graduate School of Medicine, University of Yamanashi, Yamanashi 409-3898, Japan. ✉email: hamada-n@criepi.denken.or.jp; a.nakashima@yamanashi.ac.jp; yhigashi@hiroshima-u.ac.jp

VE-cadherin	Vascular endothelial cadherin
VSMC	Vascular smooth muscle cell

Exposure of humans to ionizing radiation affects the circulatory system depending on the level of dose[1]. Radiation-induced increases in vascular permeability underlie various early effects that occur in a few days after exposure, such as skin erythema (e.g., > 3 Gy), salivary grand swelling (e.g., > 8 Gy), and lethality from cardiovascular/central nervous system syndrome (e.g., > 50 Gy)[2]. Subsequently, radiation-induced vascular stenosis leads to ulcers and necrosis in various tissues[3]. Late effects that occur in years to decades after exposure include ischemic heart disease and stroke (e.g., > 0.5 Gy)[4]. For these radiation effects on the circulatory system, the large blood vessels (e.g., the aorta) have been among the proposed critical target tissues[4,5]. For radiation protection of the circulatory system, justification and optimization of radiation exposure would be indispensable in planned exposure scenarios from controlled radiation sources (e.g., for medical or occupational exposure). However, unplanned exposure scenarios from uncontrollable radiation sources exist (e.g., unintentional accidents or intentional malicious events leading to nuclear and radiological incidents)[6]. Because radiation exposure cannot be known in advance of the incidents, medical countermeasures against radiation effects of unplanned exposure (i.e., agents that are effective when administered after radiation exposure) need to be developed as part of public health preparedness. Such agents remain unavailable, in contrast to significant efforts made to develop radioprotective agents that are effective when administered prior to radiation exposure (e.g., free-radical scavengers and anti-oxidants)[7,8].

Mesenchymal stem/stromal cells (MSCs) are multipotent adult tissue stem cells with low immunogenicity and high potential for self-renewal and multidirectional differentiation, e.g., into vascular endothelial cells (VECs) and vascular smooth muscle cells (VSMCs)[9]. The therapeutic potential of MSCs in the context of radiation injury was first demonstrated in preclinical models, wherein systemically administered MSCs contributed to tissue regeneration, the attenuation of inflammation, and improvement in survival outcomes following total body irradiation[10,11]. The study by François et al. provided compelling evidence suggesting that intravenous MSC infusion could restore hematopoietic function and improve survival after lethal irradiation in mice. Similarly, Chapel et al. reported that gene-modified MSCs expressing anti-apoptotic factors provided radioprotection to multiple organ systems, reinforcing the multifaceted therapeutic usefulness of MSCs in radiation syndromes[12]. Preclinical studies have recently shown promise for MSC-based cell therapy or to treat radiation injury in various tissues (e.g., in the brain, oral mucosa, lung, heart, intestine and liver)[13], but such therapeutic potential has not been tested in the large blood vessels. Using our recently developed model to induce vascular damage in the aorta of mice with sublethal dose of radiation[14], we set out to investigate whether post-irradiation implantation of human MSCs restore radiation-induced vascular damage.

Results

Irradiation causes vascular damage in the aorta

The aorta collected at four weeks after acute irradiation underwent the FE-SEM analysis (Fig. 1) to evaluate morphological changes to immunofluorescence and histochemistry staining to assess cellular and molecular changes (Figs. 2, 3 and 4). In the tunica intima, irradiation induced detachment of the endothelium (Fig. 1Ad), decreases in endothelial waviness (Fig. 1Ac and 1B), e-NOS (Figs. 2A and 3C) and VE-cadherin (adherence

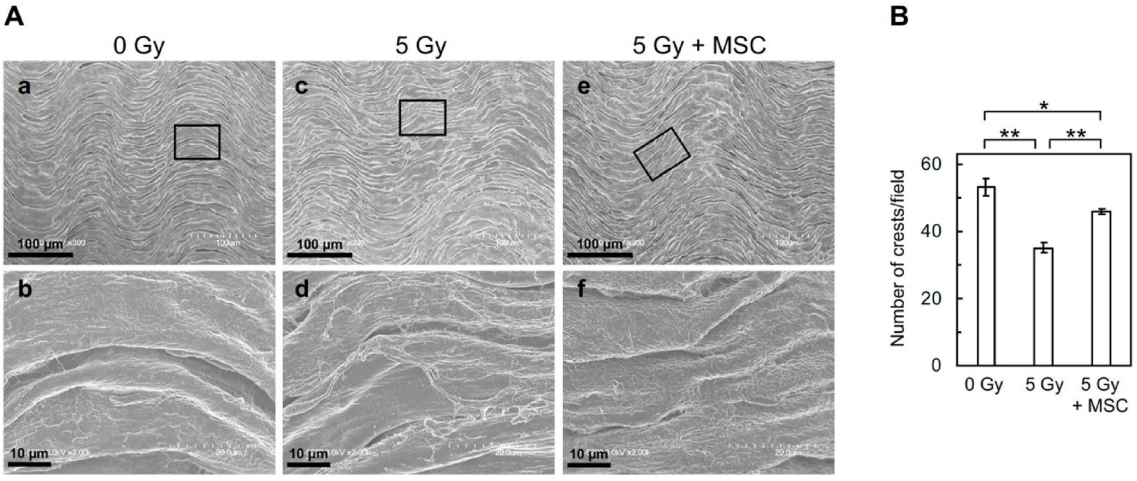

Fig. 1. Mesenchymal stem cell (MSC) implantation reduces radiation-induced morphological changes in the aorta.**A**, Representative images of field-emission scanning electron microscopy (FE-SEM) for morphology of aortic endothelium. Mice were irradiated with 0 Gy (**a**) or 5 Gy (**b**, **c**), and injected with MSCs (**c**) or vehicle (**a**, **b**) at 6 h after irradiation. All images were taken at 4 weeks after irradiation. Boxed areas in the upper panels are shown at higher magnification in the lower panels. Scale bars are as indicated. **B**, Quantitative analysis for the number of crests/field at 4 weeks after irradiation. All data are presented as means ± SE ($n = 8$/group). p by Wilcoxon rank sum test (**, $p < 0.01$; *, $0.01 \leq p < 0.05$, after Bonferroni corrections).

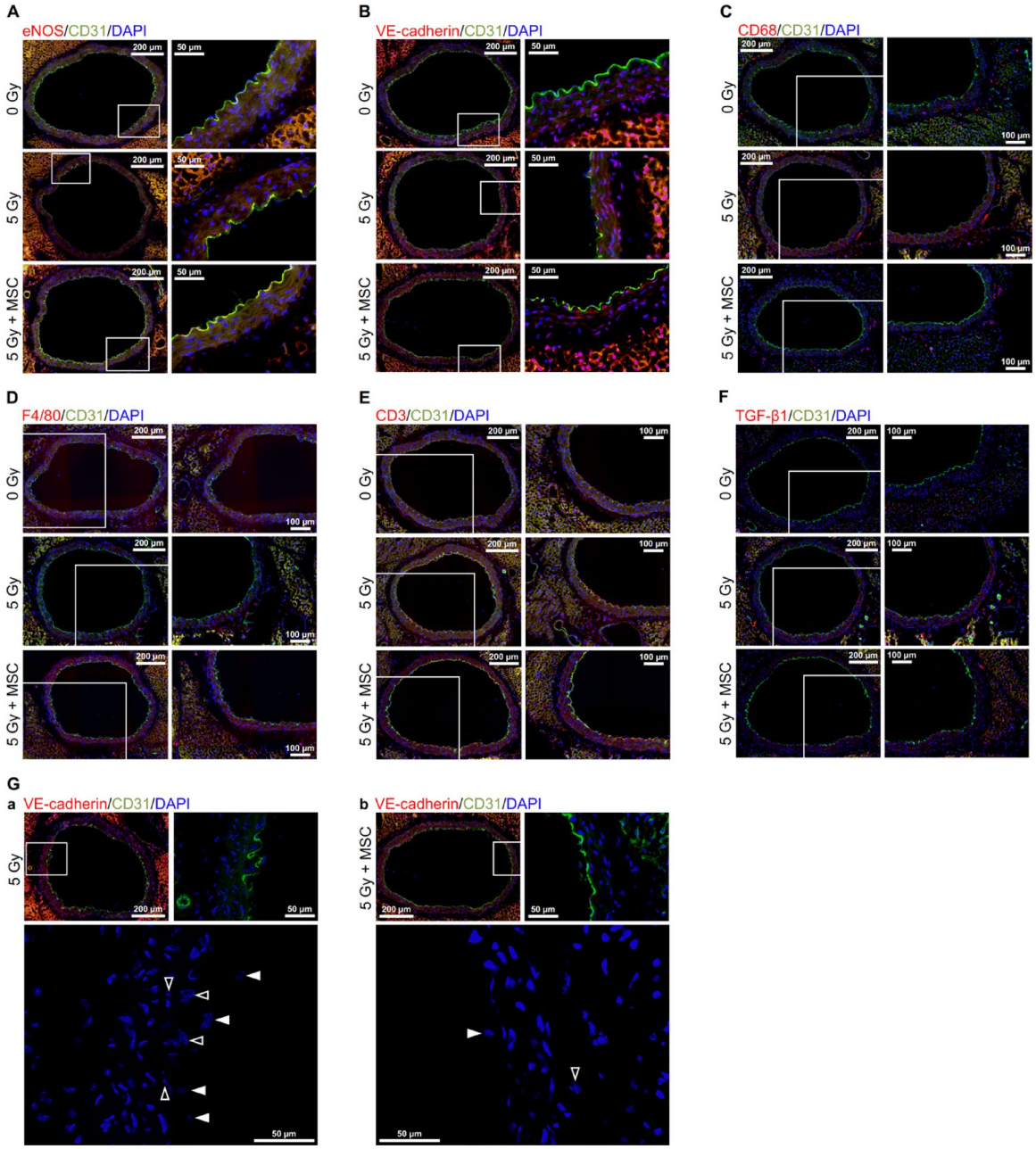

Fig. 2. Representative immunofluorescence images for molecular changes in the aorta.**A** through **F**, Representative images for CD31 (green) with (**A**) eNOS, (**B**) VE-cadherin, (**C**) CD68, (**D**) F4/80, (**E**) CD3 or (**F**) TGF-β1 (red), with cell nuclei counterstained with DAPI (blue). Mice were irradiated with 0 Gy (upper panels) or 5 Gy (middle and lower panels), and injected with MSCs (lower panels) or vehicle (upper and middle panels) at 6 h after irradiation. All images were taken at 4 weeks after irradiation. Boxed areas in the left panels (tiled images) are shown at higher magnification in the right panels. Scale bars are as indicated. **G**, Representative images for aortic cells with subcellular fragments. Mice were injected with MSCs (**b**) or vehicle (**a**) at 6 h after irradiation with 5 Gy. All images were taken at 4 weeks after irradiation. Boxed areas in the upper left panels (tiled images) are shown at higher magnification in other two panels, with the upper right panels further enlarged in the lower panels: the upper left panels are for VE-cadherin, CD31 and DAPI, the upper right panels for CD31 and DAPI, and the lower panels for DAPI. Closed and open arrowheads in the lower panels point to vascular endothelial cells with subcellular fragments in the tunica intima and vascular smooth muscle cells with subcellular fragments in the tunica media, respectively. Scale bars are as indicated. For quantitative data, see Fig. 4.

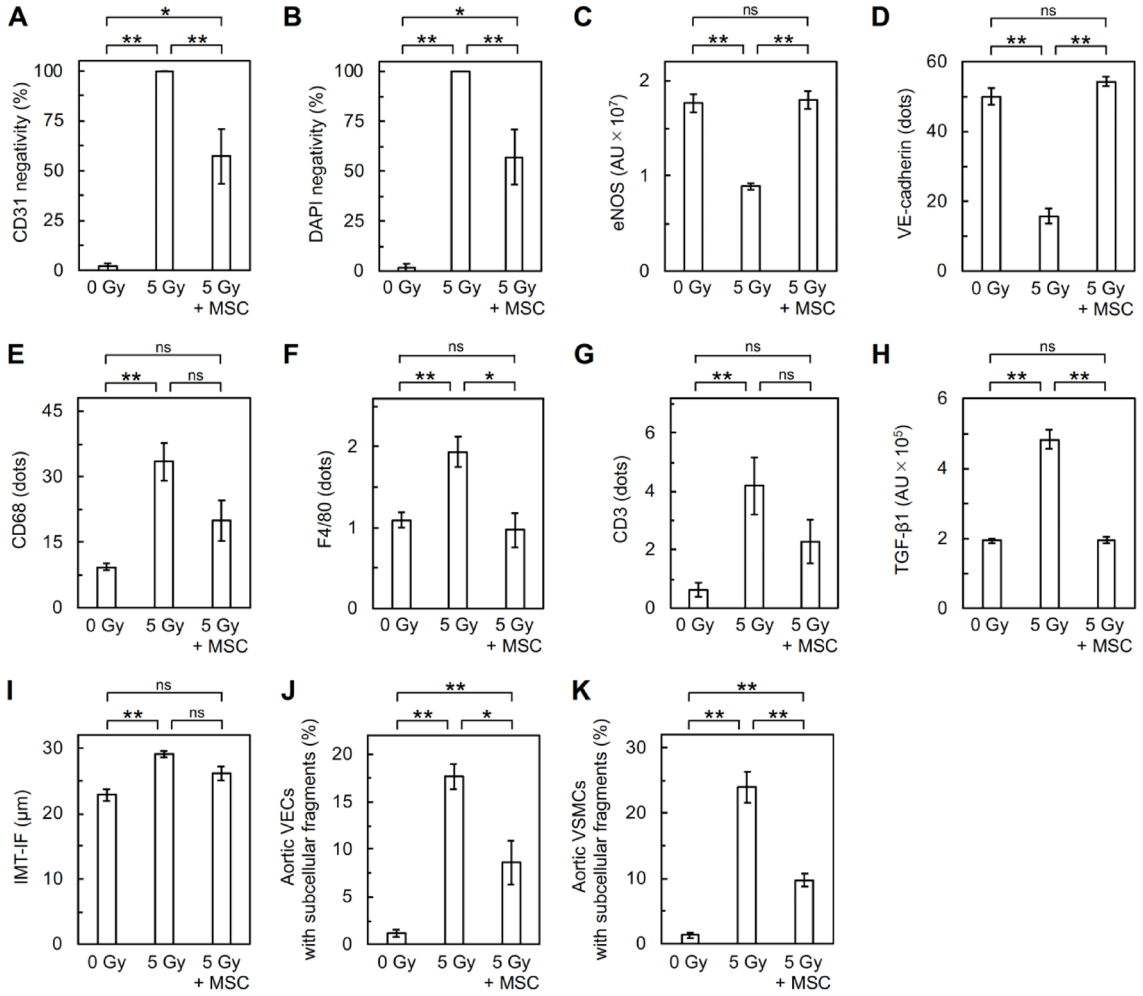

Fig. 3. Mesenchymal stem cell (MSC) implantation reduces radiation-induced vascular damage and inflammation in the aorta.**A** through **K**, Quantitative analysis of immunofluorescence images for (**A**) CD31 negativity, (**B**) DAPI negativity, (**C**) eNOS, (**D**) VE-cadherin, (**E**) CD68, (**F**) F4/80, (**G**) CD3, (**H**) TGF-β1, (**I**) IMT-IF, (**J**) vascular endothelial cells (VECs) with subcellular fragments, and (**K**) vascular smooth muscle cells (VSMCs) with subcellular fragments. Mice were injected with MSCs or vehicle at 6 h after irradiation with 0–5 Gy, and the aorta was obtained for immunofluorescence staining at 4 weeks after irradiation. All data are presented as means ± SE ($n = 8$/group). p by Wilcoxon rank sum test (**, $p < 0.01$; *, $0.01 \le p < 0.05$; ns, $p \ge 0.05$, after Bonferroni corrections). AU, arbitrary unit. For representative immunofluorescence images, see this figure.

junction protein, Figs. 2B and 3D), increases in VEC death (Figs. 2G and 3J, and partial loss of the endothelium manifested as loss of signals of CD31 (Fig. 3A) and DAPI (Fig. 3B). These results indicate that irradiation causes partial loss of the aortic endothelium, which is mediated by VEC death. In the tunica media, irradiation resulted in increases in macrophage markers (CD68 and F4/80, Figs. 2C and D and 3E and F), a T-cell marker (CD3, Figs. 2E and 3G), a pro-fibrosis marker (TGF-β1, Figs. 2F and 3H), a fibrosis maker (collagen, Fig. 4A and B), IMT (Figs. 3I and 4C), and VSMC death (Figs. 2G and 3K). These results indicate that irradiation leads to VSMC death, inflammation, macrophage recruitment, fibrosis and intima-media thickening.

MSC implantation mitigates radiation-induced vascular damage in the aorta

To examine whether MSC implantation mitigates radiation-induced vascular damage, MSCs obtained from Human adipose tissue were intravenously injected at 6 h after irradiation, and The aorta collected at four weeks after irradiation was subjected to the FE-SEM analysis, immunofluorescence and histochemistry staining. MSC implantation fully prevented radiation-induced changes in eNOS, VE-cadherin, F4/80, TGF-β1, fibrosis and IMT (Figs. 3C, D and H and 4B and C), where the level of damage in the 5 Gy + MSC group was lower than the 5 Gy group, and not different from the 0 Gy group. MSC implantation alleviated radiation-induced changes in endothelial waviness, endothelial loss, VEC death and VSMC death (Figs. 1B and 3A, B, J and K), where the level of damage in the 5 Gy + MSC group was lower than the 5 Gy group, but higher than the 0 Gy group. These results indicate that MSC implantation mitigate radiation-induced vascular damage.

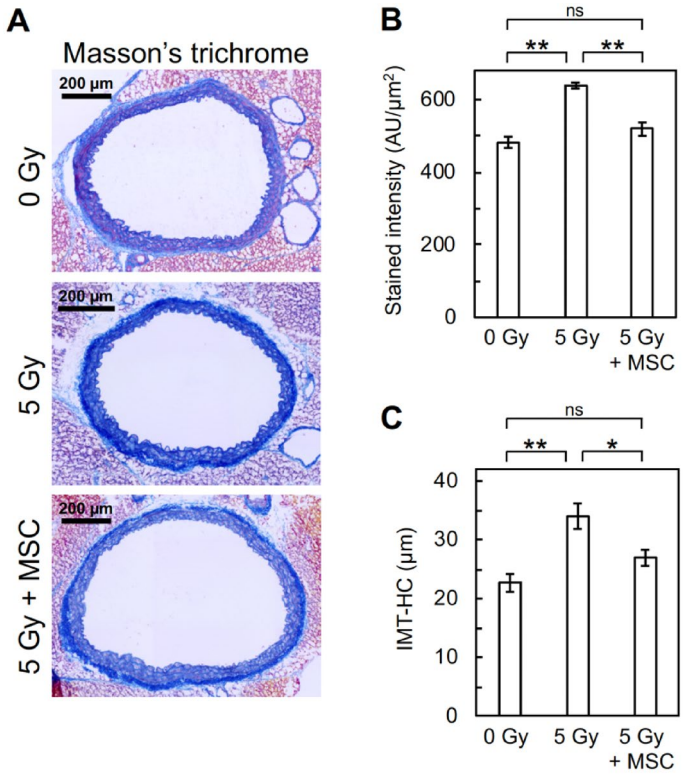

Fig. 4. Mesenchymal stem cell (MSC) implantation reduces radiation-induced fibrosis in the aorta.**A**, Representative images for Masson's trichrome staining. Scale bars are as indicated. **B** and **C**, Quantitative analysis of fibrotic alterations for (**B**) intensity of alanine blue, and (**C**) IMT-HC. Mice were injected with MSCs or vehicle at 6 h after irradiation with 0–5 Gy, and the aorta was obtained for Masson's trichrome staining at 4 weeks after irradiation. All data are presented as means ± SE ($n = 8$/group). p by Wilcoxon rank sum test (**, $p < 0.01$; *, $0.01 \leq p < 0.05$; ns, $p \geq 0.05$, after Bonferroni corrections). AU, arbitrary unit.

Observation of lethality following 5 Gy irradiation

No lethality was observed in any group throughout the 30-day observation period. All animals survived until the designated endpoint, confirming that 5 Gy was indeed a sublethal dose under our experimental conditions.

Discussion

Here, we have demonstrated that post-irradiation implantation of human adipose tissue-derived MSCs mitigate radiation-induced vascular damage in the murine aorta.

Injected MSCs are known to sense tissue damage caused by radiation insults or other toxic threats, migrate into the target tissue, differentiate into VECs for example, and release a regenerative secretome in an effort to preserve tissue homeostasis[15]. Our results obtained from in vivo experiments with MSCs and mice (Figs. 1, 2, 3 and 4) are in line with the observation in a rat model of radiation injury in the lung that MSCs derived from rat subcutaneous adipose tissue exhibited anti-inflammatory, anti-fibrosis and anti-apoptotic effects when intravenously injected at 2 h after thoracic irradiation with 15 Gy of X-rays[16].

We contextualized our findings within this established framework by emphasizing that, unlike the aforementioned studies that primarily focused on systemic or hematopoietic recovery, our study extends the scope of MSC-based radioprotection to the vascular system, specifically the aorta[10–12,17]. We suggested that the observed mitigation of endothelial dysfunction, vascular remodeling, and inflammation by MSC therapy in our model represents an important and previously underexplored dimension of the efficacy of MSCs Moreover, by using a sublethal localized radiation dose and focusing on subacute vascular pathology, our study provides a complementary perspective to the survival-focused paradigms of earlier investigations[10–12,17]. We believe that the inclusion of these landmark references not only strengthens the scientific grounding of our study but also confirms its novelty and relevance in the continuum of MSC-based radioprotective research.

Some possible mechanisms by which MSC implantation mitigated radiation-induced vascular damage in the murine aorta are hypothesized. MSCs exhibit potent anti-apoptotic effects across a variety of injury and disease models. These effects are largely attributed to paracrine signaling, including the release of trophic factors that inhibit apoptosis in damaged or stressed cells such as endothelial cells, cardiomyocytes, neurons, or epithelial cells[18,19]. MSCs also secrete cytokines and growth factors such as vascular endothelial growth factor (VEGF), hepatocyte growth factor (HGF), insulin-like growth factor-1 (IGF-1), and stromal cell-derived factor-1 (SDF-1)[18–20]. These factors then activate the survival pathways such as PI3K/Akt, ERK1/2, and STAT3, which in turn suppress the apoptotic signaling cascades[19,21]. MSC-derived factors are known to reduce the expression

or activation of caspase-3, caspase-8, and caspase-9, which are considered key executioners of apoptosis[19,20]. Moreover, MSCs tend to increase the expression of Bcl-2, Bcl-xL, and other anti-apoptotic proteins in recipient cells[19–21]. MSCs help preserve mitochondrial membrane potential and prevent cytochrome c release, which is a critical step in the intrinsic apoptotic pathway[19,22]. The anti-apoptotic pathway provides only a partial view of the complex mechanisms through which MSCs exhibit their protective effects. However, it was suggested that paracrine mediators, such as exosomes and microRNAs (miRNAs), represent important complementary and potentially upstream regulators of cellular apoptosis and tissue repair[23]. MSCs may function predominantly via paracrine signaling, particularly through the secretion of exosomes and extracellular vesicles enriched in regulatory miRNAs, proteins, lipids, and other bioactive factors[23]. Helissey et al. reported that MSC-derived exosomes can carry miRNAs such as miR-21, miR-126, and miR-146a, which have been implicated in suppressing apoptosis, modulating inflammatory responses, and promoting endothelial survival after radiation or oxidative stress[24]. These miRNAs are also known to target key pro-apoptotic mediators, including PTEN, Bim, and p53, and may thus provide a molecular link between MSC paracrine activities and anti-apoptotic outcomes[24,25]. Future research should analyse the roles of the MSC anti-apoptotic pathway in the improvement of radiation-induced vascular injuries; conduct quantitative and qualitative analyses of the MSC secretome, including exosome isolation and characterization; and perform miRNA profiling of both secreted exosomes and target endothelial tissues and the functional validation of exosome-mediated anti-apoptotic effects using gain- and loss-of-function strategies (e.g., miRNA mimics/inhibitors or exosome-depletion protocols). By incorporating this broader mechanistic context, we aim to more accurately reflect the multifaceted nature of MSC therapy and to identify concrete directions for future research aimed at elucidating the paracrine regulatory networks that underlie MSC-mediated radioprotection.

Unmodified MSCs, while promising, may exhibit limited efficacy under certain pathological conditions, and several strategies have been established to improve their reparative and immunomodulatory properties[26,27]. These approaches involve exposing MSCs to specific stimuli, such as hypoxia, inflammatory cytokines (e.g., interferon-γ, tumor necrosis factor-α), toll-like receptor agonists, or pharmacological agents, prior to administration to improve their survival, homing efficiency, and secretion of regenerative factors[27,28]. Several studies have shown that preactivated MSCs exhibit superior therapeutic efficacy compared with naïve MSCs in the models of tissue injury, including radiation-induced damage[28,29]. For instance, preconditioning with inflammatory cytokines has been shown to upregulate the expression of anti-inflammatory molecules (e.g., indoleamine 2,3-dioxygenase, prostaglandin E2) and adhesion molecules (e.g., intercellular adhesion molecule 1, vascular cell adhesion molecule 1, C-X-C motif chemokine receptor 4), thereby improving the immunosuppressive potency and tissue-targeting capacity of MSC[28,30]. Hypoxic preconditioning has also been shown to increase MSC resistance to oxidative stress and augment the release of angiogenic and cytoprotective factors[29]. We referenced relevant studies demonstrating these approaches and noted that while our study used naïve, unmodified MSCs, future studies should investigate whether preactivation or gene modification strategies may further improve the outcomes in radiation-induced vascular injury. This is particularly relevant in settings wherein systemic inflammation or oxidative stress might impair MSC viability and therapeutic action[26,29].

Immune profiling is essential when evaluating the safety and efficacy of xenogeneic cell therapies in immunocompetent hosts. Although we did not perform comprehensive immunophenotyping analyses, such as the quantifying T cell subsets, determining macrophage polarization status, or profiling cytokine/chemokine expression, no histological evidence suggestive of acute immune rejection (e.g., perivascular or parenchymal inflammatory cell infiltration, tissue necrosis, or fibrosis) was observed in the MSC-treated aortae. This suggests that, at least within the 30-day observation period, the xenogeneic human MSCs did not elicit overt immunological rejection in immunocompetent murine recipients. This finding is consistent with the well-documented immunomodulatory properties and low immunogenicity of human MSCs, which have been shown to suppress host immune responses through several mechanisms, such as the inhibition of T cell proliferation, modulation of dendritic cell maturation, and secretion of anti-inflammatory cytokines (e.g., transforming growth factor-β, interleukin-10)[31]. Notably, several previous studies have reported the feasibility of using human MSCs in xenogeneic murine models without the need for immunosuppression[32,33]. Nevertheless, we acknowledge that the absence of the histological signs of rejection does not preclude more subtle or delayed immune responses. The use of xenogeneic MSCs remains a potential confounding factor, particularly regarding the interpretation of long-term vascular remodeling and immune–endothelial interactions. Moreover, further research is needed to investigate the use of syngeneic or allogeneic murine MSCs to eliminate xenogeneic immune confounders and detailed immune profiling (e.g., flow cytometry, single-cell RNA-seq), and time-course analyses to delineate the early versus delayed immune effects. These efforts will help establish the immunological dynamics of MSC therapy and validate the translational relevance of our findings.

Limitations

There are a number of study limitations. First, in this study, we injected MSCs cultured in serum-free medium: this was because these they were found to possess higher therapeutic potential than MSCs cultured in serum-containing medium[34]. Combination with other proposed approaches such as pre-treatment of MSCs with melatonin[35], photobiomodulation[36], or lipopolysaccharides[37] may further increase MSCs' therapeutic potential to mitigate radiation-induced vascular damage. Instead of MSCs in itself, cell-free approaches through administration of MSC-CM[13–39], extracellular vesicles or exosomes from MSC-CM[37–42] have also been shown to exhibit therapeutic effects for radiation injury in various tissues. These encourage further studies.

Second, assessing the in vivo fate of the transplanted MSCs would provide important insights into their mechanism of action. However, the primary aim of the present study was to assess the early histopathological response of the irradiated aorta following MSC administration rather than to map systemic cell trafficking. While previous studies have shown that intravenously administered MSCs tend to accumulate transiently in the

lungs and other filtering organs[43,44], increasing evidence has suggested hat their therapeutic effects are largely mediated through paracrine signaling rather than persistent engraftment at target sites[45]. This paradigm has been supported by studies reporting comparable outcomes between MSC transplantation and the administration of MSC-derived exosomes[46]. Future research using labeling strategies (e.g., fluorescent, bioluminescent, or radioactive tracers) to track MSC localization, persistence, and interaction with vascular tissues following radiation exposure is needed[43,47].

Third, an evaluation of syngeneic murine MSCs would draw a more specific conclusion concerning the roles of MSCs in the protective effects on radiation-induced vascular injure. Unfortunately, the culture of murine MSCs has been proven to be extremely challenging, and we were unable to obtain a sufficient number of cells for experimental use.

Forth, both statistical power and biological generalizability are critical for the robustness and translational value of the preclinical findings[48]. With regard to the sample size, we acknowledge that a group size of $n = 8$ per condition may compromise the ability to detect subtle but biologically relevant differences, particularly for endpoints characterized by inter-individual variability. Our sample size was determined based on previous studies on radiation-induced vascular injuries using similar histological and molecular endpoints, wherein a sample size of $n = 6–10$ per group yielded statistically significant findings[49,50]. Nonetheless, increasing the sample size to $n = 10–15$ would enhance statistical power and reduce the risk of type II error[48]. In particular, those involving functional readouts or survival analyses, should incorporate larger cohorts. With regard to sex bias, we recognize the importance of including both male and female animals in accordance with the current NIH and ARRIVE guidelines for sex as a biological variable[48,51]. In the present study, only male mice were used to reduce the variability in vascular responses that can arise from hormonal cycling in females[52]. However, we fully acknowledge that this design limits the generalizability of our findings. Future studies should include both sexes to investigate potential sex-specific effects of radiation injury and MSC therapy[48,51].

Fifth, in the present study, we selected a single sublethal dose of 5 Gy based on previously published murine models demonstrating that this dose reliably induces sustained but non-lethal vascular injury, including endothelial dysfunction, intima-media thickening, and low-grade inflammation, without confounding systemic toxicity or lethality[53]. The use of a higher radiation dose of over 8 Gy would more closely mimic the severity of tissue injury observed in therapeutic or accidental radiation exposure scenarios and would allow the assessment of MSC efficacy under conditions of more extensive endothelial damage and fibrosis. However, in murine models, whole-body exposure to ionizing radiation at doses exceeding 8 Gy is uniformly lethal, with all animals succumbing within 28 days post-irradiation[54]. The 4-week (30-day) endpoint was chosen to capture subacute pathophysiological changes, such as vascular remodeling and apoptosis, which are known to emerge within this time frame following irradiation[53]. Furthermore, longer-term observations (e.g., 8–12 weeks or beyond) are necessary to assess the durability of the MSC-mediated effects, evolution of chronic vascular lesions, and potential late-onset toxicities.

Sixth, the present study focused primarily on the histological markers of vascular damage but did not assess the physiological outcomes such as hemodynamic parameters, vascular compliance, or endothelial-dependent vasodilation[55,56]. Future functional studies are needed employing pressure–volume loop analysis, echocardiography, and isolated vessel assays[55,56]. Furthermore, we acknowledge the need for unbiased molecular profiling (e.g., RNA-seq, mass spectrometry-based proteomics) to reveal upstream regulators and broader biological pathways involved in MSC-mediated vascular protection[57,58].

Finally, survival efficacy represents a pivotal outcome measure, particularly when assessing the translational potential of therapeutic strategies aimed at mitigating radiation-induced damage in the context of public health emergencies or radiological/nuclear incidents[59]. Indeed, long-term survival and functional recovery are ultimately the most clinically relevant endpoints when assessing the effectiveness of any countermeasure in radiation injury models[60]. However, the primary objective of the present study was to characterize the subclinical and subacute vascular alterations induced by ionizing radiation and to assess the capacity of MSCs to improve these early pathophysiological changes. We intentionally selected a sublethal radiation dose (5 Gy) and a 30-day endpoint to focus on endothelial dysfunction, intima-media remodeling, and inflammatory/fibrotic changes in the absence of overt lethality[61]. This design allowed us to capture the therapeutic window during which early intervention might prevent the progression to irreversible vascular damage and downstream cardiovascular complications. However, we acknowledge that the absence of survival data and long-term follow-up represents an important limitation in the present study. Although our results provide histological and molecular evidence of MSC-mediated vascular protection in the subacute phase post-irradiation, these observations do not confirm a definitive therapeutic benefit without accompanying data on survival and functional outcomes[10]. Future studies are needed to confirm the longitudinal survival analysis following higher or fractionated radiation doses that more closely mimic real-world radiation exposure scenarios[60], comprehensive functional assessments (such as vascular compliance, blood pressure measurements, and echocardiographic parameters)[56], and evaluation of multi-organ outcomes and systemic toxicity profiles to establish safety and efficacy over extended timeframes[62].

Conclusions

In conclusion, our present data showed that post-irradiation implantation of human adipose tissue-derived MSCs can mitigate radiation-induced vascular damage in the murine aorta. Further studies are warranted to enhance therapeutic potential of MSCs for public health preparedness and medical countermeasures against unplanned radiation exposure.

Methods

Animals

Male C57BL/6J mice were purchased at 7 weeks of age from Jackson Laboratory Japan (Shiga, Japan), and acclimated for a week prior to irradiation experiments. Mice were maintained under a 12-h light/dark cycle (light onset at 8 am) with ad libitum access to food (a normal-fat diet, ~3.5 kcal/g, ~13% of the calorie from crude fat, MF obtained from Oriental Yeast, Japan) and water. All animal experiments were approved by the Animal Experimentation Committee of Hiroshima University (Approval No.: A22-21) and were conducted in accordance with the institutional and national guidelines for the care and use of laboratory animals in Japan. In addition, all animal procedures are reported in compliance with the ARRIVE guidelines. At the end of the experiments, mice were euthanized by cervical dislocation following an overdose of isoflurane. This procedure was performed in accordance with a pre-approved protocol.

MSC preparation

In all experiments, MSCs cultured in serum-free STK2 medium (Kanto Reagents, Tokyo, Japan) up to passage 4 were used, based on our finding that MSCs cultured in serum-free medium possessed higher anti-apoptotic potential than those in serum-containing medium[34]. All methods involving human tissue were carried out in accordance with relevant guidelines and regulations, including the Declaration of Helsinki. MSCs were isolated from adipose tissue obtained from patients undergoing elective breast reconstruction surgery. Regarding MSC characterization, it was confirmed that the human adipose-derived MSCs used in the present study were obtained from a certified clinical-grade cell processing facility and conformed to the minimal criteria defined by the International Society for Cellular Therapy, including plastic adherence under standard culture conditions, the expression of characteristic surface markers (positive for CD73, CD90, and CD105 and negative for CD14, CD34, CD45, and HLA-DR), and capacity for trilineage differentiation into adipogenic, chondrogenic, and osteogenic lineages in vitro. The study protocol was reviewed and approved by the Ethics Committee of Hiroshima University (Approval No: E-1516). Written informed consent was obtained from all participants prior to tissue collection. All samples were anonymized before analysis to ensure the confidentiality of donor information.

Animal irradiation, MSC treatment and tissue sampling

Just prior to irradiation, unanesthetized mice ($n=8$/group) at age 8 weeks were placed in a 12-compartment pie cage (Natsume Seisakusho, Japan), and total body irradiated with a single acute dose of 5 Gy (sublethal dose) of ^{137}Cs γ-rays (662 keV) at a dose rate of 0.5 Gy/min from Gammacell 40 Exactor, as described[63]. Control mice (the 0 Gy group, $n=8$) were sham-irradiated in parallel with the test mice. Dosimetry was conducted using a Dose Ace system with radiophotoluminescent glass rods of GD-302 M and an FDG-1000 reader, all from Asahi Techno Glass Co. Ltd. (Shizuoka, Japan). At 6 h after irradiation, 200 μL phosphate-buffered saline (PBS) with 5×10^4 MSCs (the 5 Gy + MSC group, $n=8$) or without MSCs (the 5 Gy group, $n=8$) were injected through the tail vein. At 4 weeks after irradiation (viz., at age 12 weeks), mice were anesthetized with 1.5% isoflurane by inhalation at a flow rate of 2 L/min and perfused transcardially with PBS. Of the collected descending thoracic aorta, the cranial half was evaluated for morphological changes with field-emission scanning electron microscopy (FE-SEM), the caudal half being assessed for cellular and molecular changes with immunofluorescence and histochemistry staining. No mice died or appeared moribund throughout the observation period.

FE-SEM

The cranial half of the descending thoracic aorta was opened longitudinally, washed with PBS, fixed in 1% glutaraldehyde, washed with PBS, and dehydrated in an ethanol series (30%, 50%, 70%, 90%, 99.5% and 100%). The FE-SEM (Hitachi High-Technologies S-5200) was operated at 3 kV, and the entire area of the carbon-coated tissue was observed. The surface of the normal aortic endothelium exhibited less frequent horizontal waves and more frequent vertical waves (Fig. 1Aa), and the number of crests in such vertical waves was counted in each of the seven fields/mouse (each field corresponds to the entire area of the image taken at 300× magnification, 1 crest/field corresponding to ~7.5 crests/mm^2).

Immunofluorescence and histochemistry staining

The caudal half of the descending thoracic aorta was embedded in optimal cutting temperature (OCT) compound (Sakura Finetek, Japan), snap frozen (first with the cold isopentane and then liquid nitrogen), and stored at −80 °C. The tissue was transversally cryosectioned at a 5-μm thickness (Leica CM1950). The section was mounted onto a glass slide coated with 3-aminopropyltriethoxysilane (Matsunami, Japan), air-dried, and fixed in 4% paraformaldehyde.

For immunofluorescence staining, cryosections were washed with PBS, blocked with Block Ace (Yukijirushi, Japan), reacted with primary antibodies (diluted 1:100 or 1:200), washed with PBS, and reacted with secondary antibodies (diluted 1:500), with cell nuclei counterstained with 4′,6-diamidino-2-phenylindole (DAPI). Primary antibodies used were rabbit polyclonal against vascular endothelial (VE)-cadherin, CD68, CD3 and transforming growth factor β1 (TGF-β1), rabbit monoclonal against endothelial nitric oxide synthase (eNOS, Clone D9A5L) and F4/80 (Clone SP115), rat monoclonal against CD31 (CloneMEC 13.3). Secondary antibodies used were anti-rabbit IgG conjugated with Alexa Fluor 594, and anti-rat IgG conjugated with Alexa Fluor 488. The sections were simultaneously reacted with two different primary antibodies (a set of CD31 stained red and one of the five antibodies stained green), and then with two different secondary antibodies (anti-rabbit and anti-rat). Primary antibodies were purchased from Abcam (VE-cadherin, CD68, F4/80 and CD3), Cell Signaling Technology (eNOS), Sigma (TGF-β1) and BD Pharmingen (CD31), and secondary antibodies were purchased from Invitrogen. Images were captured using a Keyence BZ-9000 fluorescence microscope (Keyence, Japan),

and processed with Keyence BZ-X Analyzer. For each mouse, staining was quantified as follows: intensity of red signals in randomly selected five areas (150 μm × 50 μm) in the tunica intima in one image taken at 600× magnification for eNOS, the number of dots in the tunica intima in four images taken at 600× magnification for VE-cadherin, intensity of red signals in randomly selected five areas (50 μm × 50 μm) in the tunica media in one image taken at 200× magnification for TGF-β1, the number of dots in the entire aortic area (including the tunica adventitia) in four images taken at 200× magnification for CD68, F4/80 and CD3, and loss of signals in 7 tiled images for CD31 and DAPI. The maximal intima-media thickness (IMT) was measured in seven images taken at 200× magnification, and such IMT measured from immunofluorescence images was designated IMT-IF. For cells with subcellular fragments, all aortic VECs in the tunica intima and aortic VSMCs in the tunica media were counted at 600× magnification in two sections for each mouse (total of 172–282 VECs and 425–724 VSMCs counted/mouse in two sections each stained for VE-cadherin/CD31 with nuclei counterstained with DAPI). A tiled image for the cross section of the aortic wall was created from 30 to 60 images for each of three colors (red, green, and blue) taken at 600× magnification for eNOS and VE-cadherin, and from 8 to 12 images taken at 200× magnification for other markers.

Following the instructions from the manufacturer (Muto Pure Chemicals, Tokyo, Japan), Masson's trichrome staining was performed where aniline blue stains collagen fibers in the tunica media blue. For each mouse, one image taken at 200× magnification was used to measure the maximal IMT (designated IMT-HC), and intensity of blue signals in the tunica media and wall area (expressed as intensity of aniline blue per unit wall area).

Statistical analysis

Statistical analyses were performed using R statistical software (version 3.6.1, R Foundation, https://www.r-project.org/). Normality was assessed by the Shapilo-Wilk test. p values were determined by non-parametric tests (the Kruskal-Wallis rank sum test, followed by Wilcoxon rank sum test with Bonferroni corrections) for in vivo data. Each data point was obtained from 8 mice for in vivo data, and represents means and standard error (SE), unless otherwise specified. $p < 0.05$ was considered significant ($p < 0.01$ presented as double asterisk **, $0.01 \leq p < 0.05$ as single asterisk *.

Data availability

All data generated or analyzed during this study are available from the corresponding author upon reasonable request.

Received: 17 May 2025; Accepted: 9 September 2025
Published online: 13 October 2025

References

1. Jahng, J. W. S., Little, M. P., No, H. J., Loo, B. W. Jr & Wu, J. C. Consequences of ionizing radiation exposure to the cardiovascular system. *Nat. Rev. Cardiol.* **21**, 880–898. https://doi.org/10.1038/s41569-024-01056-4 (2024).
2. *Medical management of radiation injuries* (IAEA,).
3. Little, M. P. et al. Ionising radiation and cardiovascular disease: systematic review and meta-analysis. *BMJ* **380**, e072924. https://doi.org/10.1136/bmj-2022-072924 (2023).
4. ICRP. ICRP statement on tissue reactions/early and late effects of radiation in normal tissues and organs – threshold doses for tissue reactions in a radiation protection context. ICRP publication 118. *Ann. ICRP.* **41** (1/2), 1–322. https://doi.org/10.1016/j.icrp.2012.02.001 (2012).
5. Tapio, S. et al. Ionizing radiation-induced circulatory and metabolic diseases. *Environ. Int.* **146**, 106235. https://doi.org/10.1016/j.envint.2020.106235 (2021).
6. NCRP. Decision making for late-phase recovery from major nuclear or radiological incidents. NCRP Report No. 175. NCRP, Bethesda, Maryland.
7. Ji, L. et al. Advances of amifostine in radiation protection: administration and delivery. *Mol. Pharm.* **20**, 5383–5395. https://doi.org/10.1021/acs.molpharmaceut.3c00600 (2023).
8. Kaur, R. et al. Repurposing of various current medicines as radioprotective agents. *Anticancer Agents Med. Chem.* **23**, 1104–1121. https://doi.org/10.2174/1871520622666220404090049 (2023).
9. Lu, W. & Allickson, J. Mesenchymal stromal cell therapy: progress to date and future outlook. *Mol. Ther.* **33**, 2679–2688. https://doi.org/10.1016/j.ymthe.2025.02.003 (2025).
10. François, S. et al. Human mesenchymal stem cells favour healing of the cutaneous radiation syndrome in a xenogenic transplant model. *Ann. Hematol.* **86** (1), 1–8. https://doi.org/10.1007/s00277-006-0166-5 (2007).
11. Hu, K. X., Sun, Q. Y., Guo, M. & Ai, H. S. The radiation protection and therapy effects of mesenchymal stem cells in mice with acute radiation injury. *Br. J. Radiol.* **83** (990), 52–58. https://doi.org/10.1259/bjr/61042310 (2010).
12. Chapel, A. et al. Mesenchymal stem cells home to injured tissues when co-infused with hematopoietic cells to treat a radiation-induced multi-organ failure syndrome. *J. Gene Med.* **5** (12), 1028–1038. https://doi.org/10.1002/jgm.452 (2003).
13. Wang, K. X. et al. Mesenchymal stem cells for mitigating radiotherapy side effects. *Cells* **10**, 294. https://doi.org/10.3390/cells10020294 (2021).
14. Hamada, N. et al. Ionizing irradiation induces vascular damage in the aorta of wild-type mice. *Cancers* **12**, 3030. https://doi.org/10.3390/cancers12103030 (2020).
15. Banimohamad-Shotorbani, B. et al. DNA damage repair response in mesenchymal stromal cells: from cellular senescence and aging to apoptosis and differentiation ability. *Ageing Res. Rev.* **62**, 101125. https://doi.org/10.1016/j.arr.2020.101125 (2020).
16. Jiang, X. et al. Intravenous delivery of adipose-derived mesenchymal stromal cells attenuates acute radiation-induced lung injury in rats. *Cytotherapy* **17**, 560–570. https://doi.org/10.1016/j.jcyt.2015.02.011 (2015).
17. Sémont, A. et al. Mesenchymal stem cells increase self-renewal of small intestinal epithelium and accelerate structural recovery after radiation injury. *Adv. Exp. Med. Biol.* **585**, 19–30. https://doi.org/10.1007/978-0-387-34133-0_2 (2006).
18. Gnecchi, M., Zhang, Z., Ni, A. & Dzau, V. J. Paracrine mechanisms in adult stem cell signaling and therapy. *Circ. Res.* **103** (11), 1204–1219. https://doi.org/10.1161/CIRCRESAHA.108.176826 (2008).
19. Tang, J., Xie, Q., Pan, G., Wang, J. & Wang, M. Mesenchymal stem cells participate in angiogenesis and improve heart function in rat model of myocardial infarction. *Mol. Cell. Biochem.* **288** (1–2), 39–45. https://doi.org/10.1016/j.ejcts.2006.02.070 (2006).
20. Liu, Y. et al. Mesenchymal stem cell-based tissue regeneration is governed by recipient T lymphocytes via IFN-γ and TNF-α. *Nat. Med.* **17** (12), 1594–1601. https://doi.org/10.1038/nm.2542 (2011).

21. Shabbir, A., Zisa, D., Suzuki, G. & Lee, T. Heart failure therapy mediated by the trophic activities of bone marrow mesenchymal stem cells: a noninvasive therapeutic regimen. *Am. J. Physiol. Heart Circ. Physiol.* **296** (6), H1888–H1897. https://doi.org/10.1152/ajpheart.00186.2009 (2009).
22. Xu, J. et al. Mesenchymal stem cell-based angiopoietin-1 gene therapy for acute lung injury induced by lipopolysaccharide in mice. *J. Pathol.* **214** (4), 472–481. https://doi.org/10.1002/path.2302 (2008).
23. Ferguson, S. W. et al. The MicroRNA regulatory landscape of MSC-derived exosomes: a systems view. *Sci. Rep.* **8**, 1419. https://doi.org/10.1038/s41598-018-19581-x (2018).
24. Helissey, C. et al. Mesenchymal stem cell-derived extracellular vesicles mitigate radiation-induced damage in endothelial cells via transfer of protective MicroRNAs. *Front. Immunol.* **14**, 1145678. https://doi.org/10.3389/fimmu.2023.1145678 (2023).
25. Wang, J. et al. MicroRNA-21 protects against radiation-induced damage by targeting PTEN in bone marrow mesenchymal stem cells. *J. Cell. Physiol.* **233** (11), 9119–9129. https://doi.org/10.1002/jcp.26849 (2018).
26. Németh, K. et al. Bone marrow stromal cells attenuate sepsis via prostaglandin E2–dependent reprogramming of host macrophages to increase their interleukin-10 production. *Nat. Med.* **15** (1), 42–49. https://doi.org/10.1038/nm.1905 (2009).
27. Waterman, R. S., Tomchuck, S. L., Henkle, S. L. & Betancourt, A. M. A new mesenchymal stem cell (MSC) paradigm: polarization into a pro-inflammatory MSC1 or an immunosuppressive MSC2 phenotype. *PLoS One*. **5** (4), e10088. https://doi.org/10.1371/journal.pone.0010088 (2010).
28. English, K., Barry, F. P. & Mahon, B. P. Murine mesenchymal stem cells suppress dendritic cell migration, maturation and antigen presentation. *Immunol. Lett.* **115** (1), 50–58. https://doi.org/10.1016/j.imlet.2007.10.013 (2008).
29. Rosová, I., Dao, M., Capoccia, B., Link, D. & Nolta, J. A. Hypoxic preconditioning results in increased motility and improved therapeutic potential of human mesenchymal stem cells. *Stem Cells*. **26** (8), 2173–2182. https://doi.org/10.1634/stemcells.2007-1104 (2008).
30. Shi, M., Liu, Z. W. & Wang, F. S. Immunomodulatory properties and therapeutic application of mesenchymal stem cells. *Clin. Exp. Immunol.* **164** (1), 1–8. https://doi.org/10.1111/j.1365-2249.2011.04398.x (2011).
31. Ankrum, J. A., Ong, J. F. & Karp, J. M. Mesenchymal stem cells: immune evasive, not immune privileged. *Nat. Biotechnol.* **32** (3), 252–260. https://doi.org/10.1038/nbt.2816 (2014).
32. Eliopoulos, N., Stagg, J., Lejeune, L., Pommey, S. & Galipeau, J. Allogeneic marrow stromal cells are immune rejected by MHC class I– and class II–mismatched recipient mice. *Blood* **106** (13), 4057–4065. https://doi.org/10.1182/blood-2005-03-1004 (2005).
33. Bartholomew, A. et al. Mesenchymal stem cells suppress lymphocyte proliferation in vitro and prolong skin graft survival in vivo. *Exp. Hematol.* **30** (1), 42–48. https://doi.org/10.1016/s0301-472x(01)00769-x (2002).
34. Kadono, M. et al. Adipose-derived mesenchymal stem cells cultured in serum-free medium attenuate acute contrast-induced nephropathy by exerting anti-apoptotic effects. *Stem Cell. Res. Ther.* **14**, 337. https://doi.org/10.1186/s13287-023-03553-8 (2023).
35. Zhu, P. et al. Melatonin protects ADSCs from ROS and enhances their therapeutic potency in a rat model of myocardial infarction. *J. Cell. Mol. Med.* **19**, 2232–2243. https://doi.org/10.1111/jcmm.12610 (2015).
36. Kim, K. et al. Photobiomodulation enhances the angiogenic effect of mesenchymal stem cells to mitigate radiation-induced enteropathy. *Int. J. Mol. Sci.* **20**, 1131. https://doi.org/10.3390/ijms20051131 (2019).
37. Kink, J. A. et al. Large-scale bioreactor production of extracellular vesicles from mesenchymal stromal cells for treatment of acute radiation syndrome. *Stem Cell. Res. Ther.* **15**, 72. https://doi.org/10.1186/s13287-024-03688-2 (2024).
38. Chen, Y. X. et al. Mesenchymal stem cell-conditioned medium prevents radiation-induced liver injury by inhibiting inflammation and protecting sinusoidal endothelial cells. *J. Radiat. Res.* **56**, 700–708. https://doi.org/10.1093/jrr/rrv026 (2015).
39. Kim, Y. H. et al. Evaluation of the radiation response and regenerative effects of mesenchymal stem cell-conditioned medium in an intestinal organoid system. *Biotechnol. Bioeng.* **117**, 3639–3650. https://doi.org/10.1002/bit.27543 (2020).
40. Huang, Y. et al. Mesenchymal stem cell-conditioned medium protects hippocampal neurons from radiation damage by suppressing oxidative stress and apoptosis. *Dose Response*. **19**, 1559325820984944. https://doi.org/10.1177/1559325820984944 (2021).
41. Chen, W. et al. Characterization of cellular senescence in radiation ulcers and therapeutic effects of mesenchymal stem cell-derived conditioned medium. *Burns Trauma.* **11**, tkad001. https://doi.org/10.1093/burnst/tkad001 (2023).
42. Guo, X. et al. Exosomes of human adipose stem cells mitigate irradiation injury to salivary glands by inhibiting epithelial-mesenchymal transition through miR-199a-3p targeting Twist1 and regulating TGFβ1/Smad3 pathway. *Theranostics* **15**, 1622–1641. https://doi.org/10.7150/thno.102346 (2025).
43. Eggenhofer, E. et al. Mesenchymal stem cells are short-lived and do not migrate beyond the lungs after intravenous infusion. *Front. Immunol.* **3**, 297. https://doi.org/10.3389/fimmu.2012.00297 (2012).
44. Lee, R. H. et al. Intravenous hMSCs improve myocardial infarction in mice because cells embolized in lung are activated to secrete the anti-inflammatory protein TSG-6. *Cell. Stem Cell.* **5** (1), 54–63. https://doi.org/10.1016/j.stem.2009.05.003 (2009).
45. Gnecchi, M., Danieli, P., Malpasso, G. & Ciuffreda, M. C. Paracrine mechanisms of mesenchymal stem cells in tissue repair. *Methods Mol. Biol.* **1416**, 123–146. https://doi.org/10.1007/978-1-4939-3584-0_7 (2016).
46. Phinney, D. G. & Pittenger, M. F. Concise review: MSC-Derived exosomes for Cell-Free therapy. *Stem Cells.* **35** (4), 851–858. https://doi.org/10.1002/stem.2575 (2017).
47. Liang, X., Ding, Y., Zhang, Y., Tse, H. F. & Lian, Q. Paracrine mechanisms of mesenchymal stem cell-based therapy: current status and perspectives. *Cell. Transpl.* **23** (9), 1045–1059. https://doi.org/10.3727/096368913X667709 (2014).
48. Clayton, J. A., Collins, F. S. & Policy NIH to balance sex in cell and animal studies. *Nature* **509** (7500), 282–283. https://doi.org/10.1038/509282a (2014).
49. Boerma, M. & Hauer-Jensen, M. Preclinical research into basic mechanisms of radiation-induced heart disease. *Cardiovasc. Res.* **91** (2), 200–206. https://doi.org/10.4061/2011/858262 (2011).
50. Stewart, F. A., Seemann, I., Hoving, S. & Russell, N. S. Understanding radiation-induced cardiovascular damage and strategies for intervention. *Clin. Oncol. (R Coll. Radiol).* **25** (10), 617–624. https://doi.org/10.1016/j.clon.2013.06.012 (2013).
51. Tannenbaum, C., Ellis, R. P., Eyssel, F., Zou, J. & Schiebinger, L. Sex and gender analysis improves science and engineering. *Nature* **575** (7781), 137–146. https://doi.org/10.1038/s41586-019-1657-6 (2019).
52. Miller, V. M. & Harman, S. M. An update on hormone therapy in postmenopausal women: mini-review for the basic scientist. *Am. J. Physiol. Heart Circ. Physiol.* **313** (5), H1013–H1021. https://doi.org/10.1152/ajpheart.00383.2017 (2017).
53. Stewart, F. A., Seemann, I., Hoving, S. & Russell, N. S. Understanding radiation-induced cardiovascular damage and strategies for intervention. *Radiat. Res.* **180** (5), 471–476. https://doi.org/10.1016/j.clon.2013.06.012 (2013).
54. Farese, A. M. et al. A nonhuman primate model of the hematopoietic acute radiation syndrome plus medical management. *Health Phys.* **103** (4), 367–382. https://doi.org/10.1097/HP.0b013e318266eb4c (2012).
55. Matrougui, K. et al. Methods to evaluate vascular function: emphasis on resistance arteries of rats. *J. Cardiovasc. Pharmacol.* **57** (1), 1–7. https://doi.org/10.1097/FJC.0b013e3181fe62e0 (2011).
56. Flammer, A. J. et al. The assessment of endothelial function: from research into clinical practice. *Circulation* **126** (6), 753–767. https://doi.org/10.1161/CIRCULATIONAHA.112.093245 (2012).
57. Wang, Z., Gerstein, M. & Snyder, M. RNA-Seq: a revolutionary tool for transcriptomics. *Nat. Rev. Genet.* **10** (1), 57–63. https://doi.org/10.1038/nrg2484 (2009).
58. Aebersold, R. & Mann, M. Mass-spectrometric exploration of proteome structure and function. *Nature* **537** (7620), 347–355. https://doi.org/10.1038/nature19949 (2016).
59. Coleman, C. N. et al. Triage and treatment of mass casualty events involving radiation exposure. *Ann. Emerg. Med.* **57** (6), 540–552. https://doi.org/10.1016/j.annemergmed.2011.01.019 (2011).

60. MacVittie, T. J. et al. The hematopoietic syndrome of the acute radiation syndrome in rhesus macaques: a primate model of the human condition. *Radiat. Res.* **178** (2), 142–155. https://doi.org/10.1667/RR2878.1 (2012).
61. Boerma, M., Wang, J., Sridharan, V., Herbert, J. M. & Hauer-Jensen, M. Pharmacological induction of transforming growth factor-β1 in rat models enhances radiation injury in the intestine and reduces survival. *Radiat. Res.* **169** (4), 455–463. https://doi.org/10.1371/journal.pone.0070479 (2008).
62. Lenarczyk, M. et al. Cardiac injury after 10 Gy total body irradiation: indirect role of effects on abdominal organs. *Radiat. Res.* **180** (3), 247–258. https://doi.org/10.1667/RR3292.1 (2013).
63. Hamada, N. et al. Responses of the carotid artery to acute, fractionated or chronic ionizing irradiation, and differences from the aorta. *Sci. Rep.* **15** (1), 7712. https://doi.org/10.1038/s41598-025-92710-5 (2025).

Acknowledgements
The authors would like to thank Mses Miki Kagiya and Emi Wakisaka for technical assistance.

Author contributions
Y. H., T.U., A.N., and N.H, drafting the article and conception of this study; A.F., KI. K., M.M., A.S., and S.M., performing the in vivo and in vitro experiments; S.H. and S.Y., revising the article critically for important intellectual content.

Funding
This study was supported in part by the Japan Agency for Medical Research and Development (research project number: JP23bk0104124).

Declarations

Competing interests
The authors declare no competing interests.

Additional information
Correspondence and requests for materials should be addressed to N.H., A.N. or Y.H.

Reprints and permissions information is available at www.nature.com/reprints.

Publisher's note Springer Nature remains neutral with regard to jurisdictional claims in published maps and institutional affiliations.